Plant Physiol. (1996) 110: 689–696

# Differential Effects of Nitrogen Limitation on Photosynthetic Efficiency of Photosystems I and II in Microalgae[1]

**John A. Berges, Denis O. Charlebois[2], David C. Mauzerall, and Paul G. Falkowski***

Department of Applied Science, Brookhaven National Laboratory, Upton, New York 11973 (J.A.B., P.G.F.); and The Rockefeller University, New York, New York 10021 (D.O.C., D.C.M.)

**The effects of nitrogen starvation on photosynthetic efficiency were examined in three unicellular algae by measuring changes in the quantum yield of fluorescence with a pump-and-probe method and thermal efficiency (i.e. the percentage of trapped energy stored photochemically) with a pulsed photoacoustic method together with the inhibitor 3-(3,4-dichlorophenyl)-1,1-dimethylurea to distinguish photosystems I and II (PSI and PSII). Measured at 620 nm, maximum thermal efficiency for both photosystems was 32% for the diatom *Thalassiosira weissflogii* (PSII:PSI ratio of 2:1), 39% for the green alga *Dunaliella tertiolecta* (PSII:PSI ratio of 1:1), and 29% for the cyanobacterium *Synechococcus* sp. PCC 7002 (PSII:PSI ratio of 1:2). Nitrogen starvation decreased total thermal efficiency by 56% for *T. weissflogii* and by 26% for *D. tertiolecta* but caused no change in *Synechococcus*. Decreases in the number of active PSII reaction centers (inferred from changes in variable fluorescence) were larger: 86% (*T. weissflogii*), 65% (*D. tertiolecta*), and 65% (*Synechococcus*). The selective inactivation of PSII under nitrogen starvation was confirmed by independent measurements of active PSII using oxygen flash yields and active PSI using P700 reduction. Relatively high thermal efficiencies were measured in all three species in the presence of the PSII inhibitor 3-(3,4-dichlorophenyl)-1,1-dimethylurea, suggesting the potential for significant cyclic electron flow around PSI. Fluorescence or photoacoustic data agreed well; in *T. weissflogii*, the functional cross-sectional area of PSII at 620 nm was estimated to be the same using both methods (approximately $1.8 \times 10^2$ Å$^2$). The effects of nitrogen starvation occur mainly in PSII and are well represented by variable fluorescence measurements.**

In marine phytoplankton, nitrogen limitation affects photosynthesis by reducing the efficiency of energy collection due to loss of Chl *a* and increases in nonphotochemically active carotenoid pigments (Herzig and Falkowski, 1989; Geider et al., 1993). It also directly affects photochemical energy conversion because of decreases in protein synthesis that appear to affect chloroplastic proteins (and thus the proteins of PSI and PSII reaction centers) more strongly than cytoplasmic proteins (Rhiel et al., 1986; Kolber et al., 1988; Falkowski et al., 1989; Geider et al., 1993). There is some evidence that nitrogen deficiency affects the two photosystems differently (Rhiel et al., 1986; Kolber et al., 1988), but this has not been systematically investigated.

In intact cells, changes in photochemical energy conversion can be monitored through measurements of fluorescence emissions and heat loss. Such techniques are based on a partitioning of the light energy absorbed by cells to losses as heat, losses as fluorescence, or $E_p$; assumptions about the magnitude of the third term allow $E_p$ to be calculated from either the energy lost as fluorescence or the energy lost as heat. Both approaches have disadvantages. Fluorescence emission at ambient temperatures is almost entirely due to PSII (Krause and Weis, 1991); therefore, fluorescence cannot provide information about PSI. Processes in PSI may be particularly significant in organisms such as cyanobacteria in which PSII:PSI ratios are typically less than unity (Kawamura et al., 1979) or under conditions under which ratios of PSII:PSI change. Also, fluorescence emission represents only 2 to 5% of light energy absorbed by cells for healthy cells (Cha and Mauzerall, 1992); therefore, a minor loss term is used to estimate $E_p$. Alternatively, energy storage in both photosystems can be measured directly using time-resolved PPA (Malkin and Canaani, 1994). PPA measures the sound wave created when thermal expansion of surrounding gases occurs because of heat loss during photochemical energy transduction in the sample. Resolving differences between PSII and PSI, however, requires either excitation light that is specific to the individual photosystem or the use of selective inhibitors such as DCMU (Cha and Mauzerall, 1992).

In this study, we examined the effects of nitrogen limitation in three diverse species of algae: a diatom (*Thalassiosira weissflogii*) in which the PSII:PSI ratio was approximately 2:1, a green alga (*Dunaliella tertiolecta*) having a PSII:PSI ratio of approximately 1:1, and a cyanobacterium (*Synechococcus* sp. PCC 7002) with a PSII:PSI ratio of 1:2 (Herzig and Dubinsky, 1993). We characterized the number

[1] Research was supported by the U.S. Department of Energy under contract No. DEAC02–76CH00016 and by National Science Foundation grant No. MCB90–16973 to D.C.M. J.A.B. was supported through a Postdoctoral Fellowship from the Natural Science and Engineering Research Council of Canada.

[2] Present address: 2500 Boulevard de l'universite, Universite de Sherbrooke, PQ, J1K 2R1, Canada.

* Corresponding author; e-mail falkowsk@bnlux1.bnl.gov; fax 1–516–282–3246.

Abbreviations: $\Delta\phi_{sat}$, the maximum change in the quantum yield of fluorescence (= $F_v/F_m$); $E_p$, energy stored in the photosynthetic system; $F_m$, maximal Chl fluorescence yield, emitted when PSII centers are closed; $F_o$, minimal fluorescence yield, emitted when PSII centers are open following dark adaptation; $F_v$, variable fluorescence yield (= $F_m - F_o$); PPA, pulsed photoacoustic spectroscopy; $\sigma_{PSI}$, effective absorption cross-section of PSI; $\sigma_{PSII}$, effective absorption cross-section of PSII; TE, thermal efficiency.

of active PSI and PSII reaction centers using standard biophysical techniques and compared maximum TEs and fluorescence yields to determine where the effects of nitrogen deficiency occurred. In addition, for the diatom, we compared fluorescence and photoacoustic techniques in detail by estimating the functional absorption cross-section for PSII using both techniques.

## MATERIALS AND METHODS

The diatom *Thalassiosira weissflogii* (Gru.) Fryxell et Hasle (clone T-VIC) and the chlorophyte *Dunaliella tertiolecta* Butcher (clone DUN) were grown in 1-L semicontinuous batch cultures in artificial seawater medium (Goldman and McCarthy, 1978) enriched with f/2 nutrients (Guillard and Ryther, 1962), except that silica levels were increased to 220 $\mu$M and 1 nM selenous acid was added. Cultures were grown in continuous light (200 $\mu$E $m^{-2}$ $s^{-1}$) at 18°C and were bubbled with filtered air. The cyanobacterium *Synechococcus* sp. PCC 7002 was grown in 250-mL flasks on A+ medium (Bruce et al., 1989) at 37°C under 150 $\mu$E $m^{-2}$ $s^{-1}$ with constant shaking. Nitrogen-replete cells were maintained in logarithmic growth phase by additions of fresh medium; nitrate never decreased to less than 250 $\mu$M. Nitrogen-starved cells were allowed to deplete medium initially containing 150 $\mu$M $NO_3^-$ below detection limits and were allowed to grow into stationary phase for several days before they were sampled.

For *T. weissflogii* and *D. tertiolecta*, cell numbers and volumes were determined using a model TAII Coulter Counter (Coulter, Hialeah, FL) equipped with a population accessory and a 100-$\mu$m aperture and calibrated with latex microspheres. Chl *a* and carotenoids were measured spectrophotometrically on samples filtered onto Whatman GF/F filters and extracted in 90% aqueous acetone (Jeffrey and Humphrey, 1975). In vivo absorption spectra (375–750 nm) were determined using a DW 2C spectrophotometer (Aminco, Beverly, MA) (Dubinsky et al., 1986). Oxygen flash yields and Chl *a*:$P_{700}$ ratios were measured as described by Falkowski et al. (1981) and used to calculate Chl *a*:$O_2$, Chl *a*:PSII, Chl *a*:PSI, and the number of functional reaction centers per cell.

For both fluorescence and photoacoustic measurements, data were collected from three to six separately grown, replicate cultures over a period of several months. Subsamples from each culture were filtered onto 13-mm Millipore filters (8-$\mu$m pore size) and placed in a photoacoustic cell as described by Cha and Mauzerall (1992). A four-legged fiber-optic light pipe (common end diameter 12 mm) was fixed above the sample chamber. For both fluorescence and PPA analyses, pulsed light at 620 nm (±2.5 nm half-bandwidth) was provided by a 1-$\mu$s dye laser (model LFDL-2; Candela, Wayland, MD), using Kiton Red dye (70 $\mu$M in $CH_3OH$) through one leg. We selected 620 nm to allow significant light absorption in all three species (Fig. 1), while providing energy that would reach both PSI and PSII. For fluorescence analyses, one leg of the light pipe was attached to a xenon arc lamp, filtered through three 3-mm BG 39 glass filters (Schott, Cologne, Germany) and attenuated with neutral density filters to provide a

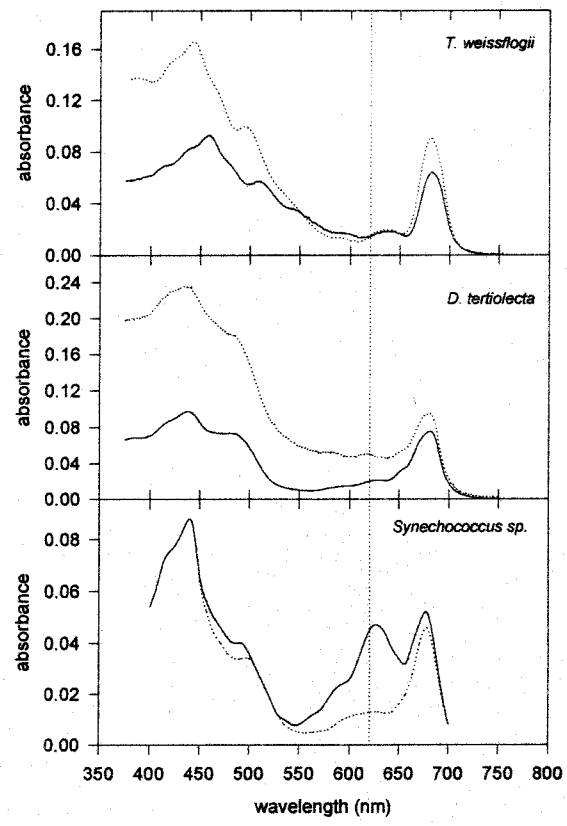


**Figure 1.** In vivo absorption spectra of *T. weissflogii*, *D. tertiolecta*, and *Synechococcus* sp. PCC 7002 under nitrogen-replete (solid lines) and nitrogen-starved (dotted lines) conditions. For *T. weissflogii* and *D. tertiolecta*, spectra are normalized to Chl *a*, determined from acetone extracts. The spectra for *Synechococcus* are taken from Bruce et al. (1989) and are in relative units. The solid line represents the nitrogen-replete state. The dashed line is for a phycobilisome-less mutant, the spectrum of which resembles the spectrum of nitrogen-starved cells. Vertical lines indicate the wavelength of laser light (620 nm) used in fluorescence yield and photoacoustic measurements.

probe flash and a third leg was directed to a 446 photomultiplier tube (Hamamatsu, Bridgewater, NJ) operated at 850 V and shielded by two 3-mm-thick heat filters, a RG 645 Schott glass filter, and a P10 720 nm band-pass filter (Corion, Holliston, MA). The photomultiplier tube current was amplified and digitized using a Hewlett-Packard high-speed digital oscilloscope connected to a 1 kΩ termination resistor. A pump-and-probe protocol was followed, whereby the fluorescence at 720 nm, elicited by a low-energy probe flash from the arc lamp, was measured before ($F_o$) and 80 $\mu$s following ($F_m$) a saturating pump flash from the laser (Mauzerall, 1972; Falkowski et al., 1986b). The intensity of the laser was then varied using a refractive attenuator, and different solutions of transition metal ions and the energy were measured at the common end of the light pipe using a radiometer (Laser Precision [Irvine, CA] Rj-7200, with a RjP-734 pyroelectric probe). Because there was significant reabsorption of fluorescence emissions with the optically dense filtered samples, maximal pump-and-probe emissions were scaled to values measured in dark-

adapted, optically thin cell suspensions using a Turner Designs (Sunnyvale, CA) model 10 fluorometer (with a Corning [Corning, NY] 5–60 filter for excitation and a Corning 2–64 filter for emission) with ($F_m$) and without ($F_o$) 20 μM DCMU. $\Delta\phi_{max}$ was calculated as the maximum $F_v/F_m$ (where $F_v = F_m - F_o$). Fluorescence measurements from the pump-and-probe method at different flash intensities ($\Delta\phi$) were fit to a simple cumulative one-hit Poisson function:

$$\Delta\phi/\Delta\phi_{max} = 1 - \exp(-\sigma_{PSII}E) \quad (1)$$

where $\sigma_{PSII}$ is the effective absorption cross-section of PSII (Å$^2$ quanta$^{-1}$ trap$^{-1}$) and $E$ is the energy of the flash. Energy transfer between PSII reaction centers was calculated by the algorithm of Ley and Mauzerall (1986), in which the parameters *a* (the probability of "escape" of a photon encountering a closed trap), *b* (the probability of escape at an open trap), and *T* (the number of traps per domain) were estimated. The results depended weakly on *b* and *T*; fixing *T* at 4.0 yielded *b* values close to 0. All curve fitting was done using the Marquardt-Levenberg method and SigmaPlot (Jandel, San Raphael, CA) for Windows version 2.0, except for the Ley and Mauzerall algorithm, which was solved using inverse methods.

PPA measurements and calculations were performed essentially as described in Cha and Mauzerall (1992). The laser flash rate was set at 3 s$^{-1}$. The photoacoustic signal, up to 120 ms, was detected in air by a microphone and filtered between 1 Hz and 10 kHz. The ratio of energy stored to total energy absorbed (corrected for the trap energy corresponding to 680 nm) (%TE) was calculated as %TE = $(H_L - H_D)/H_L \times 100\%$, where $H_L$ and $H_D$ are the acoustic signals under saturating continuous light and in the dark, respectively. Saturating continuous white light (500 μE m$^{-2}$ s$^{-1}$) was provided through the fourth leg of the light pipe (lamp model 9741–50; Cole-Parmer, Chicago, IL). Typically, it was necessary to average 50 to 200 signals to obtain a single estimate of %TE.

To estimate cross-sections of PSI, PSII activity was inhibited using DCMU. Conditions and DCMU concentration were optimized so that no variable fluorescence was detected, indicating full closure of PSII reaction centers. To eliminate variable fluorescence, it was necessary to add 150 μM DCMU to samples, mix and filter under room light, and provide a low, continuous background light (<5 μE m$^{-2}$ s$^{-1}$). Although this level of DCMU appears greatly in excess of that used in other reports and potentially above a concentration where effects are specific to PSII, the effective concentration was likely substantially lower, because in dilute cell suspensions, 20 μM DCMU was sufficient to give $F_m$ when measured in the Turner fluorometer. During the filtration process much of the DCMU may have been removed, bound by the cells, or perhaps bound to the filter itself. Control samples run under identical conditions without DCMU (but with ethanol equivalent to that in the DCMU stock) showed approximately 10% lower TE; TEs of DCMU samples were corrected for this difference. The PPA data collected with DCMU at various flash intensities were used to obtain an estimate of the cross-section of PSI using equation 7a of Cha and Mauzerall (1992):

$$TE_{PSI} = TE_{PSImax}[1 - \exp(-\sigma_{PSI}E)]/\sigma_{PSI}E, \quad (2)$$

where $TE_{PSI}$ and $TE_{PSImax}$ are the TE of PSI and the maximum TE of PSI, respectively.

Because samples were optically thick, it was necessary to correct for a baseline energy storage (Cha and Mauzerall, 1992) of 4.9% (±1.0%) in nitrate-replete and 3.0% (±1.4%) in nitrate-starved cells. Taking estimates for $TE_{PSImax}$, $\sigma_{PSI}$, and the ratio of PSII to PSI centers calculated above, we fit data collected without DCMU at different flash intensities to equations of Cha and Mauzerall (1992), assuming either linear and cyclic electron flow or linear flow alone. Fits suggested that under these conditions PSI and PSII behaved as isolated systems and trapped energy separately, so the appropriate equation is:

$$TE_{measured} = \frac{TE_{PSII}N_{PSII}[1 - \exp(-\sigma_{PSII}E)] + TE_{PSI}N_{PSI}[1 - \exp(-\sigma_{PSI}E)]}{(N_{PSI}\sigma_{PSI} + N_{PSII}\sigma_{PSII})E} \quad (3)$$

(equation 8 of Cha and Mauzerall, 1992), applying the same baseline correction as described above for the PSI curve above.

## RESULTS

Cell volume increased only slightly under nutrient starvation; thus normalizing parameters to cell numbers per-

**Table I.** *Summary of pigment and reaction center data for nitrate-replete (N-replete) and nitrate-starved (N-starved) cells of two algal species*

Values represent means of duplicate determinations from two separate cultures, and coefficients of variation are shown in parentheses.

| Parameter | *T. weissflogii* | | *D. tertiolecta* | |
|---|---|---|---|---|
| | N-replete | N-starved | N-replete | N-starved |
| Cell volume (μm$^3$) | 490 (7.9%) | 510 (8.8%) | 76 (7.4%) | 87 (8.8%) |
| Chl *a* (pg cell$^{-1}$) | 1.2 (3.5%) | 1.1 (3.4%) | 0.36 (2.1%) | 0.23 (0.6%) |
| Carotenoid:Chl *a* (mol mol$^{-1}$) | 0.60 (3.5%) | 0.88 (3.4%) | 0.68 (2.1%) | 1.7 (0.6%) |
| Chl *a*:$O_2$ (mol mol$^{-1}$) | 1130 (11.7%) | 3090 (11.5%) | 1410 (18.7%) | 2260 (9.50%) |
| Chl *a*:PSII (mol mol$^{-1}$) | 280 | 770 | 350 | 570 |
| Chl *a*:PSI (mol mol$^{-1}$) | 680 (12%) | 540 (19%) | 390 (31%) | 240 (12%) |
| PSI (mol cell$^{-1}$) (× 10$^{-19}$) | 20 | 22 | 11 | 11 |
| PSII (mol cell$^{-1}$) (× 10$^{-19}$) | 48 | 15 | 11 | 4.6 |
| PSII:PSI (mol mol$^{-1}$) | 2.2 | 0.70 | 1.1 | 0.42 |

mits a fair comparison between nitrogen-replete and nitrogen-starved cells (Table I). General effects of starvation were similar for *T. weissflogii* and *D. tertiolecta:* cell Chl *a* content declined, and the relative proportion of carotenoid increased (Fig. 1). From measurements of $P_{700}$ reduction, the number of active PSI reaction centers did not change under nitrogen starvation in either species; however, the number of active PSII centers calculated from oxygen flash yields declined to 32% of nitrogen-replete levels in *T. weissflogii* and 40% of nitrogen-replete levels in *D. tertiolecta*. The PSII:PSI ratio was 2.2 for *T. weissflogii* and 1.1 for *D. tertiolecta* when cells were nitrogen-replete, but the ratios decreased under nitrogen starvation in both species (Table I).

Fluorescence and PPA measurements were relatively insensitive to the number of cells layered on the filter for nitrogen-replete cultures, but there was an optimal amount for nitrogen-starved cells. For example, for nitrogen-replete *T. weissflogii* cultures %TE was constant between $2.5 \times 10^5$ and $2.5 \times 10^6$ cells $cm^{-2}$ of filter surface, whereas for nitrogen-starved cells the signal was maximal at $1.2 \times 10^6$ cells $cm^{-2}$, and %TE declined substantially with either smaller or larger volumes. Maximal $F_v/F_m$ ratios were lower for the cyanobacterium than for the eukaryotes (about 0.5 versus >0.65 for other species; Table II). In nitrogen-starved cells, $F_v/F_m$ ratios declined 46% for *T. weissflogii*, 40% for *D. tertiolecta*, and 24% for *Synechococcus*.

PPA measurements without DCMU represent energy storage in both PSI and PSII. These measurements indicated that between 25 and 40% of absorbed energy was stored in both photosystems, depending on the species (Table II). Under nitrogen starvation, energy storage decreased in the eukaryotes to 45% of nitrogen-replete levels in *T. weissflogii* and to 74% in *D. tertiolecta*, but no change in TE was measured in nitrogen-starved and nitrogen-replete *Synechococcus*. Addition of DCMU, under conditions that completely eliminated variable fluorescence emissions, decreased TE by 64 and 57% in *T. weissflogii* and *D. tertiolecta*, respectively, but had no significant effect in nitrogen-replete *Synechococcus* (Table II). Smaller declines were found for DCMU addition to nitrogen-starved cells: 19% for *T. weissflogii*, 41% for *D. tertiolecta*, and no change for *Synechococcus*. In all three species, nitrogen starvation had no effect on the energy storage in samples treated with DCMU (Table II).

Data obtained for active reaction centers were compared with fluorescence emission, rescaled as $F_v/F_o$ (which is assumed to be proportional to the number of active reaction centers; Falkowski et al., 1986a), or with TEs from PPA measurements in *T. weissflogii* and *D. tertiolecta*. Nitrogen starvation caused decreases in active PSII centers, measured by oxygen flash yields, which were very comparable to declines in $F_v/F_o$ in both species (Fig. 2). Similarly, declines in the sum of active PSI and PSII centers matched those in TE measured without DCMU, in which both types of reaction center contribute to the signal. More dramatic declines in total reaction centers for *T. weissflogii* than *D. tertiolecta* (to 55 and 71% of nitrogen-replete values, respectively), were matched by greater decreases in TE for *T. weissflogii* (Fig. 2). The lack of effect of nitrogen starvation on energy storage in PSI (measured by PPA in the presence of DCMU) was consistent with measurements of PSI reaction centers by absorption difference spectroscopy (Fig. 2).

Normalized variable fluorescence yield (fluorescence yield divided by the maximum yield under saturating flash energy) in nitrogen-replete *T. weissflogii* was fit better by the Ley and Mauzerall (1986) algorithm allowing energy transfer than by Equation 1 (Fig. 3). The initial lagging of the fluorescence saturation curve behind that predicted by a cummulative one-hit Poisson model, followed by a steeper increase, is commensurate with a significant level of energy transfer between reaction centers (Mauzerall and Greenbaum, 1989) (Fig. 3). The modified equation gave a cross-section of $1.7 \times 10^2$ Å$^2$ (versus $1.5 \times 10^2$ Å$^2$ using Eq. 1) and indicated a probability of 0.62 for transferring energy from a closed reaction center to another in the domain (Table III).

PPA data were highly variable between samples (coefficients of variation of approximately 25% versus approximately 3.5% for fluorescence measurements; compare Figs. 3 and 4) even when signals for 100 or more flashes per sample were averaged. For nitrogen-replete *T. weissflogii*, using PPA data obtained in the presence of DCMU, a cross-section for PSI of $5.3 \times 10^2$ Å$^2$ was calculated from Equation 2 (Fig. 4A; Table III). Substituting PSI values into Equation 3, a cross-section for PSII of $1.9 \times 10^2$ Å$^2$ was calculated (Fig. 4B; Table III), which was not significantly different from the cross-section derived using variable fluorescence data.

The same analysis was attempted using nitrogen-starved *T. weissflogii*; however, the signal-to-noise ratio for these samples was considerably poorer, particularly at low flash energies. The cross-section determined by fluorescence in-

**Table II.** *Comparisons between maximal variable fluorescence emissions and TEs in nitrate-replete and nitrate-starved cultures of three algae*

$F_v/F_m$ refers to the maximum variable fluorescence yield. TE was measured using the pulsed photoacoustic method, with or without DCMU. Values represent means of at least three separate samples, and coefficients of variation are shown in parentheses.

| Species | Nutrient Status | $F_v/F_m$ | TE | TE (−DCMU) |
|---|---|---|---|---|
| | | | % | % |
| *T. weissflogii* | Nitrogen replete | 0.71 (1.9%) | 32 (6.5%) | 11 (9.5%) |
| | Nitrogen starved | 0.38 (2.3%) | 14 (5.6%) | 12 (16%) |
| *D. tertiolecta* | Nitrogen replete | 0.67 (1.7%) | 39 (2.6%) | 17 (11%) |
| | Nitrogen starved | 0.40 (1.5%) | 29 (10%) | 17 (11%) |
| *Synechococcus* (PC 7002) | Nitrogen replete | 0.50 (6.0%) | 26 (6.1%) | 24 (0.85%) |
| | Nitrogen starved | 0.38 (4.0%) | 30 (8.9%) | 24 (8.2%) |

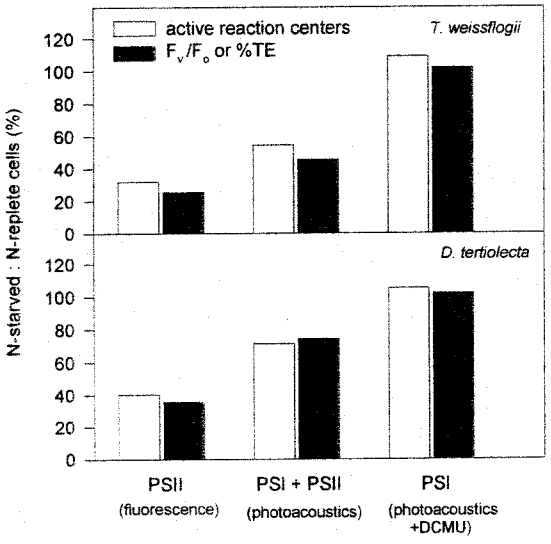


**Figure 2.** Relative numbers of active reaction centers and fluorescence yields, or %TE, of nitrate-starved versus nitrate-replete *T. weissflogii*. Active reaction centers were determined from biophysical measurements (oxygen flash yields for PSII or spectroscopically measured reduction of P700 for PSI). $F_v/F_o$ for PSII was calculated from fluorescence measurements with saturating pump flashes, and %TE was determined from pulsed photoacoustic measurements (maximum efficiency) measured at 620 nm with DCMU (PSI) or without DCMU (PSI + PSII).

creased to $4.0 \times 10^2$ Å$^2$ (Table III and data not shown). PPA data indicated a similar increase in $\sigma_{PSII}$ to $4.3 \times 10^2$ Å$^2$ (Table III and data not shown). PPA data also suggested an increase in $\sigma_{PSI}$ (data not shown).

## DISCUSSION

The most striking result of the present study is the finding that PSII is strongly affected by nitrogen starvation in the three species examined, whereas there is no apparent effect of nitrogen starvation on PSI. Our data for PSII agree with the results of other studies documenting losses of PSII reaction center proteins under continuous nitrogen limitation in chemostats (Kolber et al., 1988) and the selective degradation of PSII-serving phycobilisomes in cyanobacteria (Kana et al., 1992). However, there is less agreement concerning the effects of nitrogen starvation on PSI proteins. Plumley et al. (1989) found no changes in PSI-associated proteins in nitrogen-limited *Chlamydomonas* sp., despite a 65% decrease in certain PSII proteins, but Rhiel et al. (1986) found losses of PSI protein in nitrogen-limited *Cryptomonas maculata*. Herzig and Falkowski (1989) showed that when the chromophyte *Isochrysis galbana* was grown under increasing nitrogen limitation in chemostats the number of PSII reaction centers decreased to 56% of nitrogen-replete levels, but this was matched by losses in PSI; the PSII:PSI ratio remained almost constant at 1.6 (Falkowski et al., 1989). It is possible that the effects of nitrogen deprivation on PSI vary with species, with whether the cells are nitrogen starved versus limited by a continuous nitrogen supply as in a chemostat, or with the duration of starvation. For example, the effects of senescence on photoacoustic energy storage in pea leaves were time dependent: PSII was affected much earlier and more severely than was PSI (Gruszecki et al., 1991). For *Synechococcus*, we did not measure active reaction centers directly, as was the case for the eukaryotes. However, our results agree with those of Collier et al. (1994), who showed that in *Synechococcus* sp. PCC 7940 nitrogen deprivation decreased oxygen evolution and photoacoustically measured energy storage by 90% and yet left PSI storage relatively unaffected.

The cyanobacterium showed no apparent effect of nitrogen starvation on %TE, despite a significant decline in PSII efficiency estimated by the fluorescence technique. Although it is true that the *Synechococcus* PCC 7002 has a greater proportion of PSI than PSII, some decline in the %TE of the combined photosystems would be expected. We believe that this discrepancy is due to the wavelength at which we chose to measure PPA and fluorescence emissions. In the eukaryotes, absorption in the region of 620 nm is due to Chls *b* or *c*, which direct energy to both photosystems. In the cyanobacterium, there is a large absorption peak in this region due to phycobiliproteins, which direct energy largely to PSII (Fig. 1; Bruce et al., 1989). Under nitrogen deficiency, the phycobiliproteins are selectively degraded (Kana et al., 1992), resulting in a dramatic change in absorption at 620 nm, as demonstrated in the spectrum of a phycobilisome-less mutant (Fig. 1). We suggest that in nitrogen-deficient *Synechococcus*, energy absorbed at 620 nm is transfered toward PSI to a much greater extent than under nitrogen-replete conditions; because PSI is relatively unaffected by nitrogen deficiency, the TE does not change.

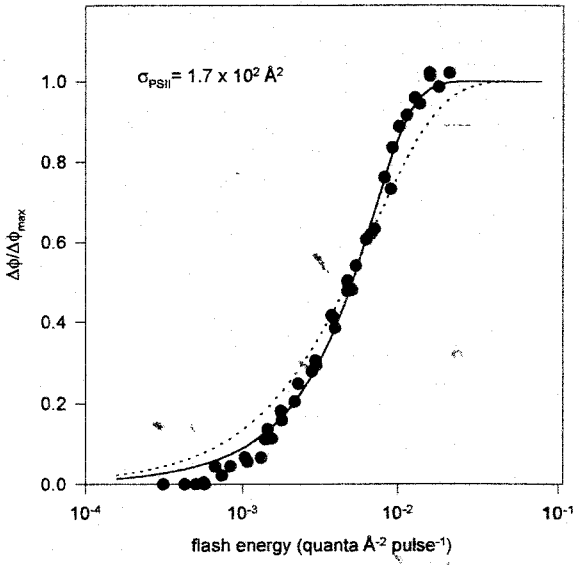


**Figure 3.** Fluorescence yield ($\Delta\phi$) normalized to maximum yield achieved under saturating flash energy ($\Delta\phi_{max}$) as a function of incident flash energy at 620 nm for nitrate-replete cultures of *T. weissflogii*. Each point represents an average of six signals. The dotted curve is the cumulative one-hit Poisson saturation function (Eq. 1), giving $\sigma_{PSII} = 1.5 \times 10^2$ Å$^2$. The solid curve was fitted using the modified algorithm of Ley and Mauzerall (1986) (see "Materials and Methods") and gives $\sigma_{PSII} = 1.7 \times 10^2$ Å$^2$. Full model parameters are given in Table III.

**Table III.** *Summary of parameters for fluorescence and photoacoustic data fit to Poisson models for T. weissflogii grown under nitrate-replete (N-replete) or nitrate-starved (N-starved) conditions*

Fluorescence parameters are for the algorithm of Ley and Mauzerall (1986) (see "Materials and Methods"). Photoacoustic parameters for PSI are from Equation 2 for data collected in the presence of DCMU (+DCMU), and these PSI parameters are then used in Equation 3 to estimate PSII parameters for data collected without DCMU (−DCMU). In both cases, TE is corrected for an apparent baseline of 4.9% in nitrogen-replete and 3.0% in nitrogen-starved cells. Asymptotic SEs are given photoacoustic fits. All measurements were made at 620 nm. –, Not applicable.

| Model | Parameter | N Replete | | N Starved | |
|---|---|---|---|---|---|
| | | −DCMU | +DCMU | −DCMU | +DCMU |
| Fluorescence | $\sigma_{PSII}$ (× $10^2$ Å$^2$) | 1.7 | – | 4.0 | – |
| | *a* | 0.62 | – | 0.50 | – |
| Photoacoustic | $TE_{PSI}$ (%) | 14 (1.4) | 14 (1.4) | 14 (4.9) | 14 (4.9) |
| | $\sigma_{PSI}$ (× $10^2$ Å$^2$) | 5.3 (1.4) | 5.3 (1.4) | 12 (4.3) | 12 (4.3) |
| | $TE_{PSII}$ (%) | 36 (1.7) | – | 13 (3.8) | – |
| | $\sigma_{PSII}$ (× $10^2$ Å$^2$) | 1.9 (0.34) | – | 4.3 (2.6) | – |

The reasons for a strong, selective effect of nitrogen starvation on PSII probably relate to the rapid turnover of D1 and D2, compared to the more stable PSI reaction center proteins (Plumley et al., 1989). Although nitrogen starvation may not change protein turnover rates, those proteins with the fastest inherent turnover rates will be most strongly affected by declines in protein synthesis due to lack of nitrogen. Plumley et al. (1989) hypothesized that decreases in PSII proteins would reduce linear electron flow and lead to relatively higher rates of cyclic photophosphorylation. This is apparently a common stress response in many photosynthetic organisms (see below). Collier et al. (1994) speculated that maintaining PSI while PSII declines is a means of preventing the production of toxic oxygen radicals that might occur if electron flow in PSII exceeded that in PSI in nutrient-deprived cells.

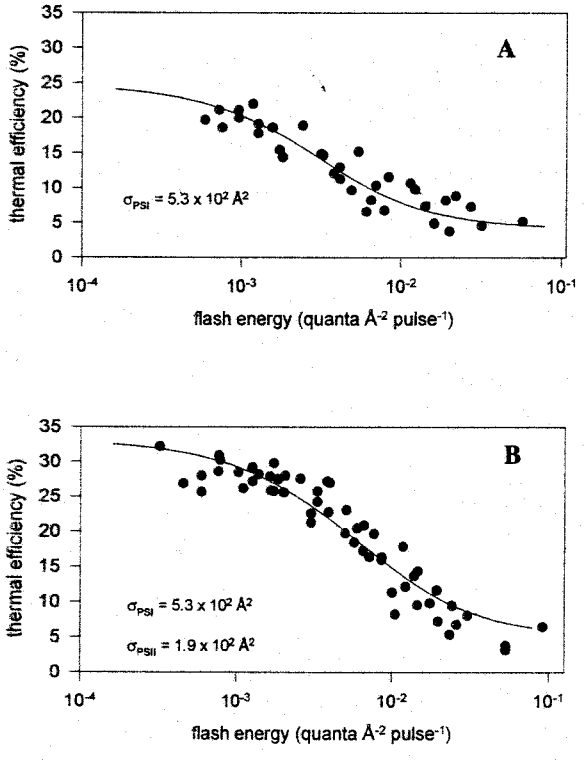


**Figure 4.** %TE measured using a pulsed photoacoustic method as a function of incident flash energy at 620 nm for nitrate-replete cultures of *T. weissflogii*. Each point represents an average of 50 or more signals from a separately prepared sample. A, Samples treated with 150 μM DCMU as described in the text and fit to Equation 2, assuming no PSII activity. This yields $\sigma_{PSI}$ = 5.3 × $10^2$ Å$^2$. B, Untreated samples fit to Equation 3, assuming the two photosystems are behaving independently under the experimental conditions. In this case, $\sigma_{PSII}$ = 1.9 × $10^2$ Å$^2$. Full model parameters are given in Table III.

Even with large decreases in active PSII centers due to nitrogen starvation or additions of DCMU, cells still showed substantial energy storage. These results indicate a relatively large capacity for cyclic electron flow. Cyclic electron flow around PSII has been found in chlorophyte algae and appears to occur in vivo (Falkowski et al., 1986a; Cha and Mauzerall, 1992). It may function to dissipate excess excitation energy and prevent photoinhibition, but it may also lead to ATP synthesis and thus be responsible for part of the energy storage observed by photoacoustic measurements. PSI cycles have frequently been documented in higher plants and algae (Fork and Herbert, 1993; Bendall and Manasse, 1995). Although such cycling is thought to be in the range of 3 to 15% of total energy storage in most cases (Fork and Herbert, 1993), it may be more significant under stresses such as photoinhibition and nutrient deprivation (Herzig and Dubinsky, 1993). It is hypothesized that cells could use ATP produced from cyclic PSI flow to repair damage to PSII that occurs under photoinhibition or to drive nutrient uptake through ATP-dependent pumps. Some types of nutrient transport, especially that of $CO_2$, phosphorus, and sulfur have been linked with PSI in cyanobacteria; PSI activity is enhanced by starvation for these nutrients (Fork and Herbert, 1993), and this may also be true for nitrogen. Cyclic photophosphorylation could be even more important in algae than higher plants, because algae do not show the same degree of carbohydrate storage as higher plants and therefore have less ability to generate ATP from storage.

Cyclic PSI electron flow may not be beneficial for all cases of nutrient deprivation. In contrast to nitrogen limitation, for cells suffering iron limitation PSI appears to be more strongly affected than PSII. Greene et al. (1991) found that in iron-starved *Phaeodactylum tricornutum* the func-

tional PSII:PSI ratio increased from 2.9 to 4.2. It would be interesting to examine energy storage in iron-starved cells. The different effects of the two nutrients may also provide a means to experimentally manipulate PSII:PSI ratios within a single species.

The data obtained using fluorescence and photoacoustic methods were internally consistent. For the eukaryotic species (*T. weissflogii* and *D. tertiolecta*), maximal fluorescence and PPA data agreed well with the independently derived data for numbers of PSI and PSII centers (Fig. 1). For the diatom, we found that photoacoustic measurements and fluorescence methods gave identical cross-sections for PSII. These results agree with some previous comparisons showing that saturation of photoacoustic and fluorescence signals seems to occur at similar light energy in spinach thylakoid membranes (Carpentier et al., 1991) and half-saturation constants for both processes are comparable in spinach PSII particles (Allakhverdiev et al., 1994) but appear to be at odds with other studies. Meaningful comparisons are made difficult by the range of different techniques (e.g. pulsed versus modulated light photoacoustics and pump-and-probe versus modulated light variable fluorescence measurements) and the variety of cell preparations used. Phenomena such as variable fluorescence saturating before TE (Malkin and Canaani, 1994) or variable fluorescence at zero energy storage (Driesenaar et al., 1994) have been reported but were not observed in the present study.

Photoacoustic methods are more variable and less sensitive compared to fluorescence techniques; eukaryotic species in particular gave highly variable PPA signals between replicates, especially at low flash intensity. Such variability appears to be a function of the species used and may relate to cell size, the way in which cells stack on the filter, or cell composition, e.g. the silica frustules formed by diatoms. Also, the eukaryotic species used in the present study were more sensitive than the cyanobacterium, particularly nitrogen-starved cells. Filtered samples could not be used for more than one measurement without significant declines in TE. In contrast, variable fluorescence emissions are a sensitive indicator of nutrient deficiency in the laboratory, and the method is amenable to field situations (Greene et al., 1991; Kolber and Falkowski, 1993). PPA does offer unique insights about PSI, however. A novel finding is that both PSII and PSI cross-sections apparently increase under nitrogen starvation. In the case of PSII, this indicates that as reaction centers become nonfunctional the pigment bed can effectively transfer excitation energy to the remaining PSII centers. For PSI, this cannot be the case because the number of PSI centers does not change. One explanation is that trapped energy is transferred from inactive PSII centers to PSI centers. In fact, Weis (1985) observed such an energy spillover in spinach leaves and noted that it increased as thylakoid membrane organization broke down at higher temperatures. Nitrogen limitation also affects thylakoid membrane structure in this way (Rhiel et al., 1986) and may facilitate such energy transfer.

It is important to recognize the limitations of both techniques used in the present study when drawing larger conclusions about photosynthetic processes. Time-resolved PPA techniques measure energy storage over a period of 2 to 20 ms; by itself this method cannot identify the storage forms of this energy, nor can it determine whether the energy is ultimately channeled toward gas exchange. Furthermore, for both methods, assumptions are needed to convert energy captured to carbon ultimately fixed. Particularly in the case of cyclic electron flows, the processes of photochemical energy storage, photosynthetic oxygen evolution, and ultimately photosynthetic carbon fixation are likely to be uncoupled.

In conclusion, the results of our study indicate that the major effects of nitrogen limitation occur in PSII. There is a clear contrast between the diatom species, which is severely affected because of its relatively abundant PSII centers, and the PSI-dominant cyanobacterium, which appears to be much less affected by nitrogen starvation. Since diatoms are abundant in nitrogen-rich coastal waters and decline quickly after nitrogen is exhausted (Guillard and Kilham, 1977), whereas cyanobacteria dominate in nitrogen-deficient open-ocean waters (Joint, 1986), it is intriguing to speculate that different photosystem stoichiometries may confer advantages to certain species and thus play a role in determining planktonic community structure.

## ACKNOWLEDGMENTS

The authors thank Ms. Irene Zelinsky for assistance with the preparation of medium and maintenance of cyanobacterial cultures and Dr. Zbigniew Kolber for help with variable fluorescence measurements and curve fitting. Comments from Dr. Jean-Marc Ducruet helped to improve the manuscript.

Received July 24, 1995; accepted November 1, 1995.
Copyright Clearance Center: 0032–0889/96/110/0689/08.

## LITERATURE CITED

**Allakhverdiev SI, Klimov VV, Carpentier R** (1994) Variable thermal emission and chlorophyll fluorescence in photosystem II particles. Proc Natl Acad Sci USA **91:** 281–285

**Bendall DS, Manasse RS** (1995) Cyclic photophosphorylation and electron transport. Biochim Biophys Acta **1229:** 23–38

**Bruce D, Brimble S, Bryant DA** (1989) State transitions in a phycobilisome-less mutant of the cyanobacterium *Synechococcus* sp. PCC 7002. Biochim Biophys Acta **974:** 66–73

**Carpentier R, Owens TG, LeBlanc RM** (1991) Simultaneous saturation of variable fluorescence yield and photoacoustically monitored thermal emission in thylakoid membranes. Photochem Photobiol **53:** 565–569

**Cha Y, Mauzerall DC** (1992) Energy storage of linear and cyclic electron flows in photosynthesis. Plant Physiol **100:** 1869–1877

**Collier JL, Herbert SK, Fork DC, Grossman AR** (1994) Changes in the cyanobacterial photosynthetic apparatus during acclimation to macronutrient deprivation. Photosynth Res **42:** 173–183

**Driesenaar ARJ, Schreiber U, Malkin S** (1994) The use of photothermal radiometry in assessing leaf photosynthesis. II. Correlation of energy storage to photosystem II fluorescence parameters. Photosynth Res **40:** 45–53

**Dubinsky Z, Falkowski P, Wyman K** (1986) Light harvesting and utilization by phytoplankton. Plant Cell Physiol **27:** 1335–1349

**Falkowski PG, Fujita Y, Ley AC, Mauzerall DC** (1986a) Evidence for cyclic electron flow around photosystem II in *Chlorella pyrenoidosa*. Plant Physiol **81:** 310–312

**Falkowski PG, Owens TG, Ley AC, Mauzerall DC** (1981) Effects of growth irradiance levels on the ratio of reaction centers in two species of marine phytoplankton. Plant Physiol **68:** 969–973

**Falkowski PG, Sukenik A, Herzig R** (1989) Nitrogen limitation in *Isochrysis galbana* (Haptophyceae). II. Relative abundance of chloroplast proteins. J Phycol **25:** 471–478

**Falkowski PG, Wyman K, Ley AC, Mauzerall DC** (1986b) Relationship of steady-state photosynthesis to fluorescence in eucaryotic algae. Biochim Biophys Acta **849:** 183–192

**Fork DC, Herbert SK** (1993) Electron transport and photophosphorylation by photosystem I in vivo in plants and cyanobacteria. Photosynth Res **36:** 149–169

**Geider R, La Roche J, Greene R, Olaizola M** (1993) Response of the photosynthetic apparatus of *Phaeodactylum tricornutum* (Bacillariophyceae) to nitrate, phosphate, or iron starvation. J Phycol **29:** 755–766

**Goldman JC, McCarthy JJ** (1978) Steady state growth and ammonium uptake of a fast growing marine diatom. Limnol Oceanogr **23:** 695–703

**Greene RM, Geider RJ, Falkowski PG** (1991) Effect of iron limitation on photosynthesis in a marine diatom. Limnol Oceanogr **36:** 1772–1782

**Gruszecki WI, Veeranjaneyulu K, Zelent B, LeBlanc RM** (1991) Energy transfer process during senescence: fluorescence and photoacoustic studies of intact pea leaves. Biochim Biophys Acta **1056:** 173–180

**Guillard RR, Ryther JH** (1962) Studies on marine plankton diatoms. 1. *Cyclotella nana* Hustedt and *Dentonula confervacae* (Cleve) Gran. Can J Microbiol **8:** 229–239

**Guillard RRL, Kilham P** (1977) The ecology of marine diatoms. *In* D Werner, ed, The Biology of Diatoms. Blackwell Scientific, Oxford, UK, pp 372–469

**Herzig R, Dubinsky Z** (1993) Effect of photoacclimation on the energy partitioning between cyclic and non-cyclic photophosphorylation. New Phytol **123:** 665–672

**Herzig R, Falkowski PG** (1989) Nitrogen limitation in *Isochrysis galbana* (Haptophyceae). I. Photosynthetic energy conversion and growth efficiencies. J Phycol **25:** 462–471

**Jeffrey SW, Humphrey GW** (1975) New spectrophotometric equations for determining chlorophylls a, b, $c_1$, and $c_2$ in higher plants, algae and natural phytoplankton. Biochem Physiol Pflanz **167:** 191–194

**Joint IR** (1986) Physiological ecology of picoplankton in various oceanographic provinces. Can Bull Fish Aquat Sci **214:** 287–309

**Kana TM, Feimel NL, Flynn LC** (1992) Nitrogen starvation in marine *Synechococcus* strains: clonal differences in phycobiliprotein breakdown and energy coupling. Mar Ecol Prog Ser **88:** 75–82

**Kawamura M, Mimuro M, Fujita Y** (1979) Quantitative relationship between two reaction centers in the photosynthetic system of blue-green algae. Plant Cell Physiol **20:** 697–705

**Kolber Z, Falkowski PG** (1993) Use of active fluorescence to estimate phytoplankton photosynthesis *in situ*. Limnol Oceanogr **38:** 1646–1665

**Kolber Z, Zehr J, Falkowski P** (1988) Effects of growth irradiance and nitrogen limitation on photosynthetic energy conversion in photosystem II. Plant Physiol **88:** 923–929

**Krause GH, Weis E** (1991) Chlorophyll fluorescence and photosynthesis: the basics. Annu Rev Plant Physiol Plant Mol Biol **42:** 313–349

**Ley AC, Mauzerall D** (1986) The extent of energy transfer among photosystem II reaction centers in *Chlorella*. Biochim Biophys Acta **850:** 234–248

**Malkin S, Canaani O** (1994) The use and characteristics of the photoacoustic method in the study of photosynthesis. Annu Rev Plant Physiol Plant Mol Biol **45:** 493–526

**Mauzerall D** (1972) Light-induced changes in *Chlorella*, and the primary photoreactions for the production of oxygen. Proc Natl Acad Sci USA **69:** 1358–1362

**Mauzerall D, Greenbaum NL** (1989) The absolute size of a photosynthetic unit. Biochim Biophys Acta **974:** 119–140

**Plumley FG, Douglas SE, Switzer AB, Schmidt GW** (1989) Nitrogen-dependent biogenesis of chlorophyll-protein complexes. *In* WR Briggs, ed, Photosynthesis. AR Liss, New York, pp 311–329

**Rhiel E, Krupinska K, Wehrmeyer W** (1986) Effects of nitrogen starvation on the function and organization of the photosynthetic membranes in *Cryptomonas maculata* (Cryptophyceae). Planta **169:** 361–369

**Weis E** (1985) Light- and temperature-induced changes in the distribution of excitation energy between photosystem I and photosystem II in spinach leaves. Biochim Biophys Acta **807:** 118–126